

Engineering Conferences International ECI Digital Archives

5th International Conference on Porous Media and
Their Applications in Science, Engineering and
Industry

Refereed Proceedings

Summer 6-26-2014

Wall thickness optimization of a transpiration-cooled sharp leading edge at atmospheric re-entry

Christian Dittert

German Aerospace Center (DLR) - Institute of Structures and Design - Space System Integration, christian.ditter@dlr.de

Follow this and additional works at: http://dc.engconfintl.org/porous_media_V



Part of the [Materials Science and Engineering Commons](#)

Recommended Citation

Christian Dittert, "Wall thickness optimization of a transpiration-cooled sharp leading edge at atmospheric re-entry" in "5th International Conference on Porous Media and Their Applications in Science, Engineering and Industry", Prof. Kambiz Vafai, University of California, Riverside; Prof. Adrian Bejan, Duke University; Prof. Akira Nakayama, Shizuoka University; Prof. Oronzio Manca, Seconda Università degli Studi Napoli Eds, ECI Symposium Series, (2014). http://dc.engconfintl.org/porous_media_V/42

This Conference Proceeding is brought to you for free and open access by the Refereed Proceedings at ECI Digital Archives. It has been accepted for inclusion in 5th International Conference on Porous Media and Their Applications in Science, Engineering and Industry by an authorized administrator of ECI Digital Archives. For more information, please contact franco@bepress.com.

WALL THICKNESS OPTIMIZATION OF A TRANSPIRATION-COOLED SHARP LEADING EDGE AT ATMOSPHERIC RE-ENTRY

Christian Dittert, Hannah Böhrk and Hendrik Weihs

German Aerospace Center (DLR) - Institute of Structures and Design - Space System Integration,
christian.dittert@dlr.de, Stuttgart, 70569, Germany

ABSTRACT

The purpose of this paper is to find the necessary cooling mass flow for a defined wall thickness distribution, which allows a selective cooling for an acceptable temperature range of the sharp leading edge of an atmospheric re-entry vehicle. Due to the angle of attack during the re-entry flight the pressure at the top side is lower than the pressure at the bottom side. However, the highest heat load occurs at the stagnation point at which also the maximum pressure is effective. The efficiency of a transpiration cooling depends on the mass flow rate of the coolant. The cooling mass flow is therefore determined by the pressure difference between the ambient and reservoir pressure. Thus, the coolant mass flow increases if the pressure difference between the reservoir and ambient pressure increases. If so a vehicle dives into earth atmosphere, the maximum coolant mass flow is expected in a higher atmosphere. In particular, the cooling effect on the surface caused by the different pressures between top side and bottom side will be considered in more detail. These different pressures are resulting from oblique shocks caused by an angle of attack with $\alpha=5^\circ$. A possibility to compensate this effect is to adapt the wall thickness so that the coolant mass flow is constant over the transpiration cooled surface, or higher on the hot side. For this purpose the numerical code Heat Exchange Analysis for Transpiration-cooling Systems (HEATS) will be adapted to compute the temperature distribution for a defined transpiration cooled leading edge geometry and trajectory. The results are showing, for a constant mass flow for top side and bottom side, a temperature difference of about 500K at the surface, only caused by the angle of attack. In addition, the impact to the reservoir pressure is higher than 0.5bar, if the cooling mass flow is assumed as constant.

INTRODUCTION

As a research project of the German Aerospace Center (DLR), the SHarp Edged Flight EXperiment (SHEFEX) program promotes the development of new cost-effective heat shields for re-entry bodies.

The approach being pursued for a low-cost TPS system is a faceted heat shield, which is made of ceramic matrix composites. After the successful suborbital flights of SHEFEX I and II, the preparations for a SHEFEX III flight have started in 2013. The goal is to increase the heat load and the velocity compared to SHEFEX II.

As a result of the new faceted design, the sharp leading edge becomes a critical part. Hence, it is necessary to examine this part in detail. Just as for SHEFEX I and II fiber reinforced ceramics shall provide the basics of the thermal protection system. The material combination C/C-SiC, which was used for SHEFEX I and II, especially shows a successful performance of a ceramic matrix composite (CMC) sharp leading edge with a radius <1 mm for re-entry at Mach numbers between 6.5 and 10. The SHEFEX II flight at high velocity was recorded and transmitted data down to an altitude of 30 km to a ground station. A thermocouple just 20 mm behind the leading edge measured a temperature of 1121K at this trajectory point and temperatures above 2275K are suspected at altitudes below that [1].

However, the heat load expected for SHEFEX III is much higher than that for the last SHEFEX mission. As a result, new materials and cooling concepts for the thermal protection system have to be considered. A possible solution to face these high heat loads was investigated during SHEFEX II flight. The AKTiV experiment on SHEFEX II cooled down the material by transpiration cooling. For this purpose nitrogen flows through a porous C/C tile. Initial results of the flight data indicate a significant cooling effect [2].

Hence, it is planned to protect the nose of SHEFEX III by transpiration cooling. To achieve this Nose Experiment by Transpiration cooling (NEXT), it is necessary to first recognize, the differences between a plate and a wedge flow. However, during a re-entry flight, aerodynamic effects have an impact on the efficiency of the transpiration cooling, especially the pressure gradient between the top and bottom sides. This is caused by the angle of attack leading to a varying coolant rate along the surface. The pressure gradient is also influenced by the local heat transfer along the surface. To ensure that the coolant mass flow passes to

the thermally high loaded areas, the wall thickness needs to be adjusted.

This paper introduces the SHEFEX-III mission and its boundary conditions, a presentation of the equations used to determine the heat transfer, an overview about the numerical lay out tool HEATS, and its functioning. The results of this investigation include an estimation of the wall thickness, coolant mass flow, pressure distribution in the wall, and taking into account practicability.

NOMENCLATURE

T	=	temperature
t	=	time
p	=	pressure
u	=	velocity
c_p	=	heat capacity
k_D	=	Darcy coefficient
kf	=	Forchheimer coefficient
h	=	heat transfer coefficient
q	=	heat flux
Gc	=	Area specific mass flow

Greek Symbols

α	=	angle of attack
Θ	=	deflection angle
λ	=	thermal conductivity
ρ	=	density
μ	=	viscosity

Subscripts

top	=	top side
bot	=	bottom side
solid	=	solid material
fluid	=	coolant
vol	=	volumetric
x	=	grid coordinate in flow direction
y	=	grid coordinate perpendicular to flow

1 MISSION PROFILE AND BOUNDARY CONDITIONS

Contrary to the conventional blunt leading edge, like those commonly used for re-entry, sharp leading edges offer advantages in aerodynamic performance. They are known to induce minimum drag, require low thrust during ascent and achieve high cross-range during re-entry which leads to larger re-entry windows. However, they are exposed to strong aerothermodynamic loads. The shock formed ahead of the vehicle upon re-entry into the atmosphere stands ahead of blunt shapes but may be attached to pointed shapes. Blunt bodies are therefore commonly used in order to increase the shock distance from the thermal protection system (TPS) and reduce the thermal load. However, the recent progress in material development and the improvement of layout and design calculation methods allows for a reconsideration of sharp leading edge concepts for hypersonic flight.

Development of a feasible concept is, among other objectives, pursued in the re-entry flight program SHEFEX.

1.1 SHEFEX-III

SHEFEX-III is the third evolutionary stage of the SHEFEX program. Contrary to its predecessors, where among other topics the faceted thermal protection system was investigated, for SHEFEX III a lifted-body concept will be tested. The actual shape of SHEFEX-III is shown in Fig 1.



Figure 1: SHEFEX-III

In the current configuration, SHEFEX-III has an approximate mass of 500 kg and a length of about 2.0 meters. Because the development of SHEFEX leads towards orbital re-entry, an increase of the thermal loads between SHEFEX-II and III becomes a necessary next step. This increase in thermal loads can be achieved by adjusting the re-entry trajectory.

1.2 Trajectory

One investigated trajectory for SHEFEX-III is presented in Fig 2. This trajectory is characterized by an entrance speed of 5.5 km/h at 100km altitude with a remaining flight time of 800s [3]. In addition two different angles of attack should be shown in this trajectory. In the first phase, a high angle of attack is shown for maximum lift and in the second phase a small angle of attack for a maximum lift-to-drag ratio is shown.

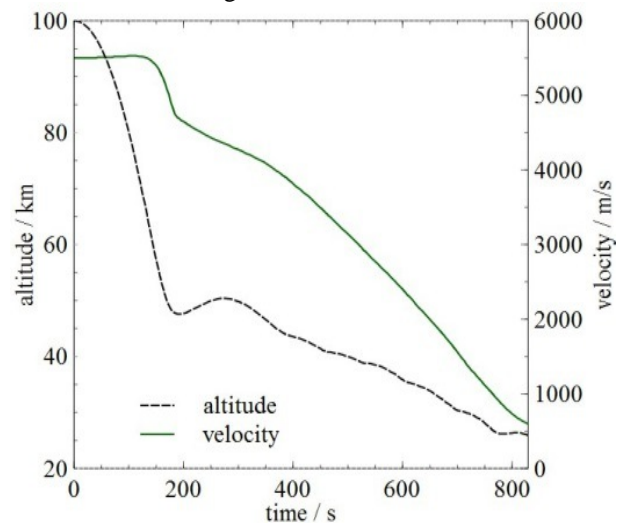


Figure 2: Trajectory [3]

In order to design a thermal protection system, it is essential to know the trajectory, because the incoming heat load during re-entry flight is particularly affected by the vehicles shape and given trajectory. By changing, for example, the re-entry velocity or the angle of attack, the heat flux can be increased or decreased.

For the following studies an angle of attack of $\alpha=5^\circ$ is selected. This leads to different flow conditions for the top side and bottom side. The oblique shock, which occurs at a given deflection angle, leads to the pressure and temperature profiles as shown for the bottom side in Fig.3 and for the top side in Fig. 4.

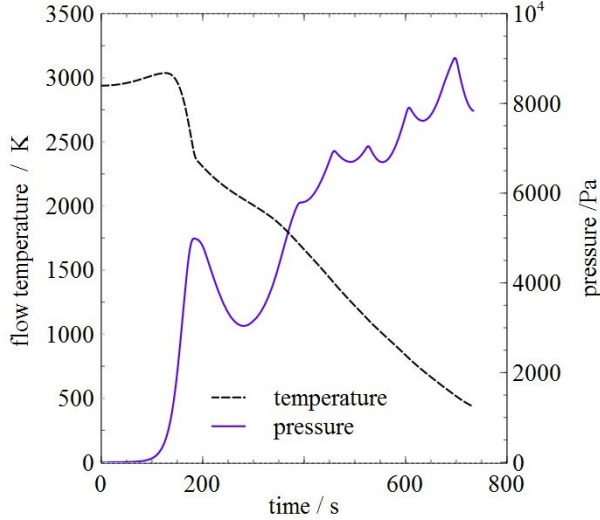


Figure 3: Flow Conditions at the Bottom Side

From the figures, it can be seen that the conditions in terms of pressure and temperature at the bottom side are significantly higher than at the top side. This difference in temperature and pressure arises from the angle of attack. The compression shock at the bottom is much stronger than the one at the top side. Therefore, the flow at the bottom side is much more compressed which leads to the high pressure and temperature increase.

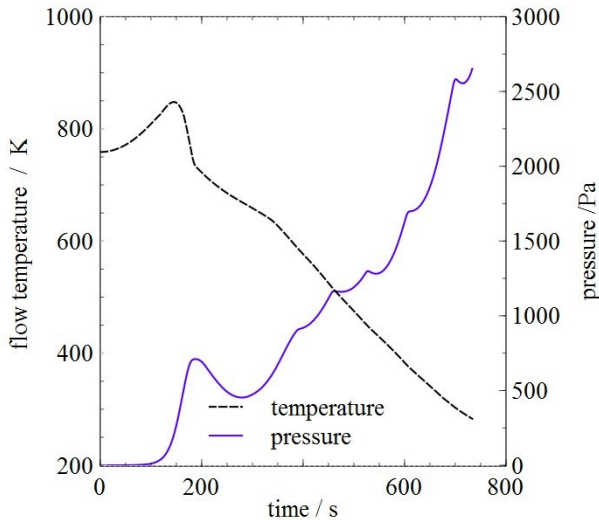


Figure 4: Flow Conditions at the Top Side

2 TRANSPIRATION COOLING AND NUMERICAL MODEL

Especially when combined with sharp leading edges which are exposed to high thermal loads in hypersonic flight, a stable material and flight condition can be achieved by using transpiration cooling.

Transpiration cooling is an active cooling method in which a fluid flows through a porous material. While the fluid flows through the material it withdraws the heat from the material. When the heated fluid arrives at the hot side of the material, it flows out and forms a cooling film which protects the material additionally from the thermal loads.

2.1 HEATS

HEATS is a semi-analytical tool for the determination of transient material temperatures along a trajectory. Therefore, it is used for preliminary design studies of thermal protection systems. In order to determine the transient wall heat flux to a material wall, HEATS solves the analytical equations for the oblique shock, and expansion fans are used to determine the state variables in the vicinity of the vehicle [4, 5]. This approach was demonstrated in a former paper and validated by comparison to the CFD-data of a particular available SHEFEX II trajectory point [6]. Furthermore, it was shown for the flight evaluation of SHEFEX-II, that the inflight wall temperatures occur just as predicted by HEATS [1]. These state variables of the atmospheric gas aerodynamically heating the surface are used as input data to HEATS.

Although HEATS can be used for the lay-out of radiation-cooled structures, the real task lies in the simulation of transpiration cooled structures. To determine the temperature distribution in the wall with HEATS, heat balances are set up and solved. In conjunction with transpiration cooling, the heat equation leads to

$$\rho_{solid} c_{p, solid} \frac{\partial T}{\partial t} = \left(\lambda_y \frac{\partial^2 T}{\partial y^2} + \lambda_x \frac{\partial^2 T}{\partial x^2} \right) + \dots \quad (1)$$

$$+ h_{vol} (T_{fluid} - T_{solid})$$

for the material. This equation is coupled with the heat equation for the fluid

$$\rho_{fluid} c_{p, fluid} \frac{\partial T}{\partial t} + G c c_{p, fluid} \frac{\partial T}{\partial y} = h_{vol} (T_{solid} - T_{fluid}) \quad (2)$$

through the volumetric heat transfer coefficient h_{vol} [7]. To determine the volumetric heat transfer coefficient, a model developed by Florio [8] is used. As a boundary condition for the heat equations (1), (2), the surface temperatures are used, which are solved via heat balances with the ambient flow. Contrary to the aerodynamic heating without transpiration cooling, where only the properties of the surrounding gas and the

material must be taken into account for the calculation, if transpiration cooling is switched on, a reduced convective heat transfer needs to be considered. Nevertheless, the heat balance of the surface can be written in the usual way as

$$\dot{q}_{convection} = \dot{q}_{conduction} + \dot{q}_{radiation} \quad (3)$$

It should be noted that for transpiration-cooling the convective heat flux on the left side is a reduced heat flux. Here a reduced heat flux is used because the cool film reduces the heat input to the material. The determination of the reduced heat flux is based on the heat exchange between the film and the surrounding flow and is described by Böhrk [4]. However, the heat transfer coefficient used to describe the convective heat flux (4) is based on known models of Crocco and van Driest [4, 8, 9].

$$h = St\rho u c_p \quad (4)$$

Here, the t heat transfer coefficient is described with the help of the flow conditions and the Stanton number. A general approach to determine the local Stanton number and the recovery factor for a laminar flow is given by van Driest [9,10] for a flat plate with the equation

$$St_x = 0.332 Pr^{-\frac{2}{3}} Re_x^{-\frac{1}{2}} \quad (5)$$

For the design of a transpiration cooled component, it is also important to know the pressure loss across the component. This is necessary to determine the reservoir pressure for given coolant mass flow. In HEATS therefore, the pressure gradient is determined after Darcy-Forchheimer [11]

$$\frac{\partial p}{\partial y} = \frac{\mu}{k_D} u + \frac{\rho}{k_F} u^2 \quad (6)$$

Because in HEATS the coolant mass flow is given, the velocity in equation (6) can be replaced by the area specific coolant mass flow. This leads to equation

$$\frac{\partial p}{\partial y} = \frac{1}{\rho} \left(\frac{\mu}{k_D} Gc + \frac{1}{k_F} Gc^2 \right) \quad (7)$$

for the pressure loss. It should be noted that a mass flow in x-direction is neglected.

2.2 Numerical Model

For this first layout a transpiration cooled inclined flat plate is considered under the boundary conditions of the top and bottom sides. This is possible because the heat transfer of an inclined flat plate comparable to the heat transfer for a wedge surface [12]. The effect of the

stagnation point on the effectiveness of the transpiration cooling is neglected in this first analysis. However, it is ensured that the top side and the bottom side are both fed by the same coolant reservoir. Thus, the boundary condition on the reservoir side for all analyses is the same.

Only those outer boundary conditions caused by the trajectory and shown in Fig. 3 and 4 are different for the top side and bottom side. Furthermore, it is assumed that the flow at the sharp leading edge is always laminar. Therefore the equations (3-5) for the heat transfer are as presented valid. As mentioned before, the model used in HEATS is a flat plate with a length of 100mm and a wall thickness of 10mm. The grid that is used to discretize the plate is shown in Fig.5. In y-direction a step size of 0.5mm is chosen, and for the x-direction a step of 0.66mm.

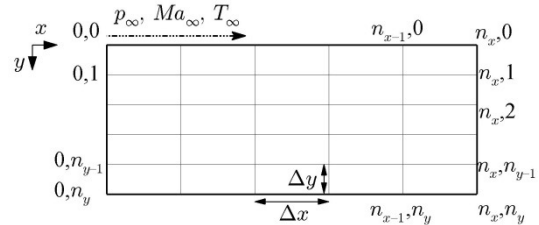


Figure 5: Grid used for a Flat Plate Model

The material for the present investigations is C/C, for which the material properties are summarized in Table 1.

Table 1. Material Properties

Material	$\lambda_{II} /$ W/mK	$\lambda_{\perp} /$ W/mK	$k_{Dj} /$ m ²	$k_{Fj} /$ m	ϵ
C/C	14	2	1.65e-13	2.9e-6	0,85

Nitrogen is used as coolant because it is assumed that it is already on board as propellant for the reaction control system. For the investigations an area specific mass flow rate of $Gc=0.1\text{kg/m}^2\text{s}$ is assumed.

3 RESULTS

In this section, the pressure and thermal responses for the material along a trajectory is shown. In addition, a locally resolved review of the material is accomplished at discrete times.

3.1 Temperature Distribution

In Fig. 6, surface temperatures for the top side and bottom side are shown. The transpiration cooling in that case was active all the time. From the figure it can be seen that the surface temperatures at the bottom side are much higher than the temperatures at the top side at the same position. It can also be seen that surface temperatures at 1/3 of the length are up to 200K higher than the temperatures at 2/3 of the length.

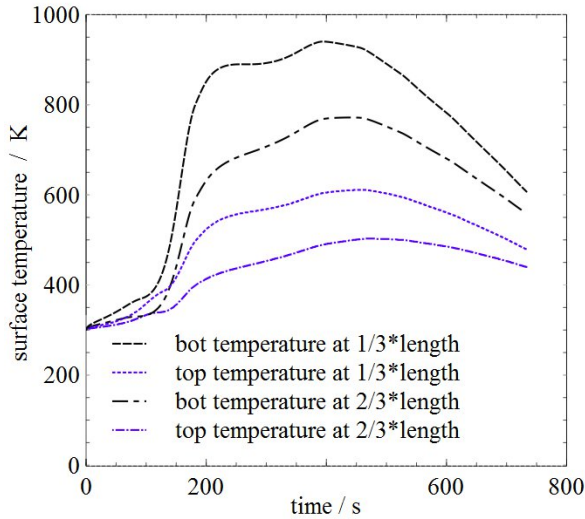


Figure 6: Surface Temperatures

This difference was expected because the convective heat transfer in accordance to equation (5) describes the local heat transfer and the Stanton number decreases with the length. Anyway, since the surface temperatures are colder than the maximum operating temperature of the material and the maximum amount of cooling gas will probably be limited, a calculation with a beginning of transpiration cooling after 150s behind re-entry start is shown in Fig.7.

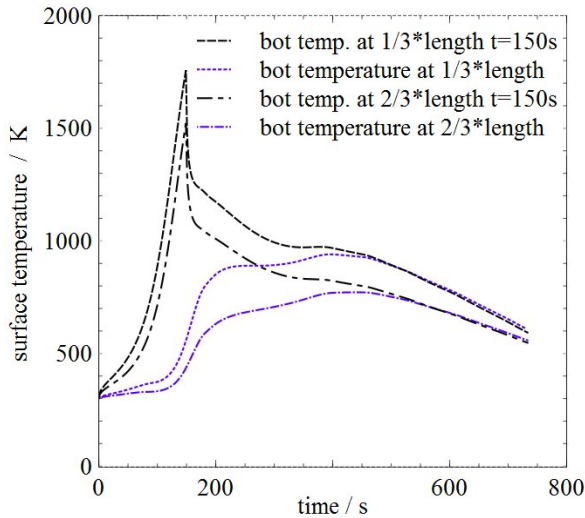


Figure 7: Surface Temperatures with different Cooling Start Times

It is apparent from the results in Fig. 7 that transpiration cooling can be used to cool down the material only during the hot phases. This is an interesting aspect when saving mass is a priority.

3.2 Pressure Distribution

The results of the pressure distribution in the material for a given coolant mass flow are particularly important for the design of the wall thickness. Especially since

specified for this paper that only one reservoir is used to supply the top and bottom sides. However, it is assumed that the pressure of the surrounding flow is imprinted on the material on the hot side. For this assumption, the pressures resulting on the cold side of the material are shown in Fig.9.

The results of the pressure profiles must be seen in relation to the results of the temperature profiles in Figure 7. It turns out that the pressure and temperature behave in a similar manner. However, when the pressure curves are considered, it must be taken into account that for a real component only one reservoir pressure would apply to the entire cold material side. The variation in the reservoir pressures is due to the constraint of having a constant coolant mass flow over the surface.

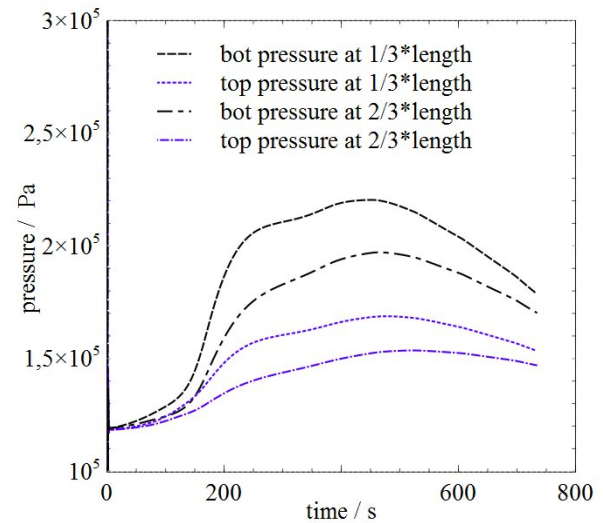


Figure 9: Reservoir Pressures

In Fig. 10 a pressure distribution among the material is shown in more detail, for a given trajectory point. The trajectory point after 200s was chosen here because there are pressure and heat peaks at this time. It turns out that the pressure in the front area is much higher than the pressure downstream. As the temperatures also decrease in the flow direction it can be assumed by a relationship of temperature and pressure. A first assumption would be that the viscosity is responsible for the change in pressure. That would be understandable because in equation (7) the temperature does not occur for the pressure calculation but the viscosity has a strong dependency from the temperature.

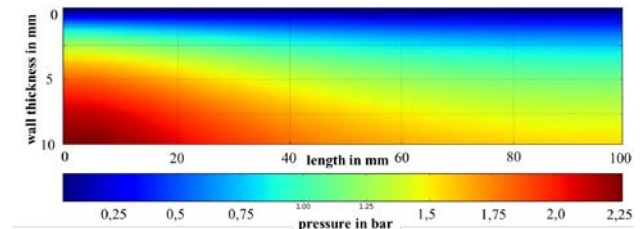


Figure 10: Pressure Distribution at t=200s

CONCLUSIONS

With regards to the optimization of wall thicknesses, the results show interesting aspects to optimize transpiration cooling. As a first major impact on the wall thickness, the different temperature distributions between the top and bottom sides were identified. It could be shown that for the same mass flow the bottom side reaches higher temperatures, due to the different flow conditions caused by the angle of attack with $\alpha=5^\circ$. Conversely, that means the cooling mass flow for the top side can be significantly reduced. However, the reduction of the mass flow seems questionable because either the wall thickness needs to be increased, or a second reservoir at a different pressure must be used. Both variants would not simplify the transpiration cooled system.

A further parameter which has a major impact on the wall thickness is shown in Fig 10. The pressure profile which arises here is the result of a constant coolant mass flow along the surface. However, the pressure profile shows that if the reservoir pressure is set constant instead of the constant coolant mass flow, then the result would be a variable coolant mass flow. This resulting mass flow would be reversed to the temperature profile, which means that the hot spots would be cooled less than the cold spots. However, if the mass flow and pressure are set to be constant, the wall thickness would vary. This wall thickness adjustment would be generated along an isobar, as can be seen in Fig.10. An adaptation of the wall thickness to smaller values especially where the highest temperatures are expected seem an incorrect place for the optimization.

Finally, there is a lot of room for optimization, but all the factors which are connected with it should be evaluated. This includes not only thermal loads but also the mechanical loads for the component.

ACKNOWLEDGEMENT

This work was supported by the Helmholtz Alliance as the Helmholtz Young Investigator's Group VH-NG-909 „High Temperature Management in Hypersonic Flight“.

REFERENCES

- [1] H. Boehrck, T. Thiele, C. Dittert, "Thermal Testing of the Sharp Leading Edge of SHEFEX II", 18th AIAA/3AF International Space Planes and Hypersonic Systems and Technologies Conference, Tours, France, Sep 2012
- [2] H. Böhrck: "Transpiration Cooling at Hypersonic Flight - AKTiV on SHEFEX II", AIAA Aviation and Aeronautics Forum and Exposition 2014, Atlanta, GA, June. 2014.
- [3] J. Telaar, H. Strauch, J. Sommer, "SHEFEX III Flight Control System," 4th International ARA-Days, Arcachon, France, Mai 2013.

- [4] H. Böhrck, O. Piol, M. Kuhn, "Heat Balance of a Transpiration-Cooled Heat Shield," Journal of Thermophysics and Heat Transfer, vol. 24, No. 3, 2010, pp. 581–588.
- [5] H. Böhrck, A. Herbertz, M. Ortelt, "Heat Balance of a Transpiration-Cooled Ceramic Combustion Chamber," Space Propulsion 2010, San Sebastian, Spain, May 2010.
- [6] H. Böhrck, M. Kuhn, H. Weihs, "Concept of the Transpiration Cooling Experiment on SHEFEX II," 2nd International ARA-Days, Arcachon, France, Oct. 2008.
- [7] M. Kaviany, "Principles of Heat Transfer in Porous Media," Springer Verlag, New York, 1991.
- [8] J. Florio, J.B. Henderson, F.L. Test and R. Hariharan "Experimental Determination of Volumetric Heat Transfer Coefficients in Decomposing Polymer Composites," Porous Media, Mixtures and Multiphase Heat transfer (ASME Winter Annual Meeting, San Francisco, CA), 1989, HTD-Vol. 117, pp. 51–60.
- [8] E.R. van Driest, "Investigation of Laminar Boundary Layer in Compressible Fluids using the Crocco Method," Tech. Rep. NACA TN-2597, NACA, 1952.
- [9] E.R. van Driest, "The Problem of Aerodynamic Heating," Aeronautical Engineering Review, Vol. 15, No. 10, 1956, pp. 26–41.
- [10] L. F. Crabtree, J. G. Woodley and R. L. Dommett, "Estimation of Heat Transfer to Flat Plates, Cones and
- [11] M. D. M. Innocenti, A. R. F. Pardo und V. C. Pandolfelli, „Modified Pressure-Decay Technique for Evaluating the Permeability of Higly Dense Refractories," *Journal of American Ceramic Society* 83, pp. 220-222, Januar 2000.
- [12] C. Dittert, H. Böhrck (2013) "Assessment of Cooling Concepts for SHEFEX III Leading Edge". 7th European Workshop on Thermal Protection Systems and Hot Structures, 8.-10. April 2013, Noordwijk, Netherlands.